

Addendum to the Proposal for a *B*-Physics Experiment at TEV I: The μ BCD

(January 7, 1991)

H. Castro, B. Gomez, F. Rivera, J.-C. Sanabria, *Universidad de los Andes*
J.F. Arens, G. Jernigan, *U.C. Berkeley, Space Sciences Lab*
P. Yager, *U.C. Davis*
J.N. Butler, L.A. Garren, S. Kwan, P. Lebrun, J. Morfin, T. Nash,
L. Stutte, *Fermilab*
P. Avery, J. Yelton, *U. Florida*
M. Adams, D. McLeod, C. Halliwell, *U. Illinois, Chicago*
R. Burnstein, H. Cease, H. Rubin, *Illinois Institute of Technology*
E.R. McCliment, Y. Onel, *U. Iowa*
D. London, *U. Montreal*
M.S. Alam, A. Deogirikar, W. Gibson, *S.U.N.Y. Albany*
C.L. Britton, K. Castleberry, C. Nowlin, C. Sohns, *Oak Ridge National Lab*
P. Gutierrez, G.R. Kalbfleisch, D.H. Kaplan, P. Skubic, J. Snow,
U. Oklahoma
L.D. Gladney, N.S. Lockyer,¹ R. Van Berg, *U. Pennsylvania*
D.J. Judd, D.E. Wagoner, K. Paick, L. Turnbull, *Prairie View A&M U.*
J.G. Heinrich, C. Lu, K.T. McDonald, *Princeton U.*
A.M. Lopez, J.C. Palathingal, A. Mendez, J. Millan, R. Palomera-Garcia,
Universidad de Puerto Rico
B. Hoeneisen, C. Marin, C. Jimenez, *Universidad San Francisco de Quito*
M. Sheaff, *U. Wisconsin*
A.J. Slaughter, E. Wolin, *Yale University*

¹Spokesperson

Executive Summary

In this Addendum to the μ BCD Proposal⁽¹⁾ we elaborate on several of the themes introduced there. In Section 2 we estimate that modifications to CDF and D0 short of implementing the μ BCD have very marginal prospects for observing CP violation. Optimum results would, of course, be obtained in an experiment dedicated to B physics, the full BCD. The μ BCD offers a physics path that could lead to the full BCD, or a B -physics experiment within the context of the existing collider program.

The critical technology in the μ BCD is the silicon vertex detector. In Sec. 3 we review the need for a 3-dimensional detector – one that measures tracks in two projections. Section 4 proposes extensions to the ongoing BCD R&D program to explore techniques of construction of the 3-D vertex detector. For this we seek a budget of \$126k, and the additional half-time support of an engineering physicist. Section 5 reviews the need for Kaon identification in a B -physics experiment, and notes that the decisive justification is the advantage of a Kaon tag over lepton tags. We close with several comments on the physics of CP violation in Sec. 6.

Contents

1	Introduction	1
2	Estimates of Sensitivity of Solenoid and Dipole Detectors to CP Violation in $B \rightarrow J/\psi K_S^0$	1
3	The Need for a 3-D Vertex Detector	4
4	Vertex Detector R&D	6
5	The Need for Kaon Identification	9
5.1	Efficiency of Lepton and Kaon Tags	9
5.2	Kaon Identification Via Mass Constraints	11
6	Comments on CP-Violation Physics	21
6.1	The Four Classes of CP Violation of Neutral B Mesons	21
6.2	The Einstein-Rosen-Podolsky Effect	22
6.3	Dilutions Due to Mixing	22
6.4	The Superweak Model	23
7	Concluding Remarks	24
8	References	25

List of Tables

1	Sensitivity of various detectors to CP violation.	2
2	Funding request for vertex R&D.	8
3	Correctly identified $B_u \rightarrow$ all-charged decays.	14
4	Incorrectly identified B_u decays.	15
5	Correctly identified $B_u \rightarrow D^0 +$ all-charged decays.	16
6	Incorrectly identified $B_u \rightarrow D^0 + X$ decays.	17
7	Correctly identified $B_d \rightarrow$ all-charged decays.	18
8	Correctly identified $B_s \rightarrow$ all-charged decays.	18
9	Correctly identified $B_d \rightarrow$ all-charged decays.	19
10	Incorrectly identified $B_d \rightarrow X$ decays.	20
11	The four classes of CP violation.	21

List of Figures

1	Figures of merit for 3-D and 2-D vertex detectors.	5
2	P_t spectra for single leptons from $B \rightarrow l^\pm X$	10
3	P_t spectrum of right-sign Kaons.	11
4	Fraction of wrong-sign leptons and Kaon <i>vs.</i> P_t	12
5	Tagging efficiency <i>vs.</i> P_t	13

1 Introduction

The Fermilab Collider B -physics program should evolve towards an experiment that can study a wide range of phenomena, including CP violation, in the late 1990's. Whether this experiment arises from CDF or D0 or is a new initiative there is a need to develop several technologies that are not emphasized in the present collider program, as they imply some compromise to the capability of top-quark searches. The three technologies are: 1) a 3-D vertex detector, 2) Kaon identification, and 3) a high-rate data-acquisition system. It will require considerable time and effort to develop these technologies, so it is important that work begin now. The μ -BCD proposal provides a near-term B -physics focus for the R&D program, which could proceed in parallel with the ongoing top-quark searches.

The ongoing R&D program (T-784) of the BCD group should include a new level of engineering studies in 1991, as discussed in Sec. 4. For this we seek a budget of \$126k, and the additional half-time support of an engineering physicist.

An immediate issue in defining the scope of B physics at Fermilab in the 1990's is whether CDF or D0 upgrades can reach CP violation in $J/\psi K_S^0$. This mode is a natural starting place for experiments since the triggering is easy. We estimate in Sec. 2 that measurement of CP violation is not possible in upgraded CDF or D0 experiments unless the asymmetry is very large and the upgrades are expanded to include Kaon identification and lepton coverage down to low P_t . Even then, the prospects for a significant measurement are very marginal.

Fermilab should support a program of B physics with a broader scope than only $B \rightarrow J/\psi X$ to include B , mixing and study of CP violation in several modes. The CP -violating asymmetries are not guaranteed to be large in any one class but must be large in at least two of four classes if the Standard Model is correct. The phenomenon of B , mixing is more accessible than CP violation and serves to test the techniques that must be developed for the latter. A capability for B , mixing requires a significant investment in triggering and data acquisition.

The μ -BCD is a better starting point for a full-range B -physics program than the proposed CDF and D0 upgrades because of its emphasis on all of the relevant technical issues, and because of its freedom from the operational constraints of the existing top-quark-search experiments.

2 Estimates of Sensitivity of Solenoid and Dipole Detectors to CP Violation in $B \rightarrow J/\psi K_S^0$

An upper limit estimate of the future capability of CDF can be made by extrapolation from the 10 or less $J/\psi K_S$ decays being studied in CDF (Internal Note only) from an exposure of 3 pb^{-1} . With no upgrades we would expect 3,300 reconstructed decays in a run of 1000 pb^{-1} . Improvements in muon coverage, and reduction in the minimum P_t cut could triple this to some 10,000 reconstructed decays.

But these must be tagged as to the particle/antiparticle character of the B at production. This can be done via the sign of the lepton in the decay of the second B to $l^\pm X$. The total semi-muonic branch is 10%, but acceptance cuts will reduce this by $\sim 1/2$, a P_t cut at 2 GeV/c will cost a factor of $1/4$, and the requirement that the muon be consistent with a

secondary vertex will reduce the tagging efficiency by another factor of $\sim 1/3$ to an overall value of about 0.5% in CDF. Hence there would be only about 50 tagged, reconstructed decays via muons that are useful for the CP -violation analysis.

With a sample of N tagged, reconstructed $B \rightarrow J/\psi K_S$ decays, the smallest CP -violating asymmetry that can be resolved to three standard deviations is about $(3 \cdot 2 \cdot 2)/\sqrt{N} = 12/\sqrt{N}$, where the factors of 2 arise from the dilutions due to mixing of both the fully reconstructed B , and of the tagging B . Thus 50 events do not allow a significant measurement of CP violation.

We have estimated the potential sensitivity of the proposed CDF upgrade, D0 upgrade, an optimal solenoidal detector for B physics (BSD), and of an optimal dipole detector (BCD) using various combinations of techniques as given in Table 1. The projections for CDF include the effect of adding Kaon identification, which has not been proposed yet.

Table 1: The numbers of tagged, reconstructed $B \rightarrow J/\psi K_S$ decays in a run of 1000 pb $^{-1}$ at CDF, at an upgraded D0, at a Bottom Solenoid Detector (BSD), and a Bottom Collider (dipole) Detector (BCD) for J/ψ decays to $\mu\mu$ and ee and for tagging of the second B via μ^\pm , e^\pm , and K^\pm . Also listed is the minimum value of the CP -violating asymmetry A that could be resolved to three standard deviations. The numbers in parentheses might be obtained in CDF with the addition of Kaon identification, which is not part of the present CDF-upgrade plan.

Technique	CDF		D0		BSD		BCD	
	Events	A_{\min}	Events	A_{\min}	Events	A_{\min}	Events	A_{\min}
μ only	50	1.00	140	1.00	140	1.00	200	0.85
e only	50	1.00	50	1.00	500	0.52	500	0.52
$\mu + e$	200	0.85	400	0.60	1200	0.35	1250	0.34
$\mu + K$	(250)	(0.76)	—	—	1400	0.32	2250	0.25
$e + K$	(250)	(0.76)	—	—	3750	0.20	4650	0.18
$\mu + e + K$	(1000)	(0.38)	—	—	5600	0.16	8400	0.13

A number of comments to Table 1 are in order:

1. We assume that the detectors would be equipped with a silicon vertex detector with both 'disks' and 'barrels' permitting 3-dimensional reconstruction of secondary vertices from B 's with low transverse momentum.
2. The muon and electron coverages in CDF are assumed to be only modest improvements over that presently planned. For equal coverage of muons and electrons the tagged, reconstructed event sample is four times as large as that for use of muons only.
3. D0 must, of course, be upgraded with a (solenoid) magnet to pursue B physics. While

D0 could evolve into the BSD, the BSD considered here has little in common with the existing D0 detector except the muon system.

4. The Bottom Solenoid Detector (BSD) represents a maximal upgrade of CDF or D0 for B physics. Although its capabilities approach those of the dipole solution (BCD) it will be more difficult technically to achieve them in the solenoid geometry.
5. The BCD is based on a transverse dipole magnet such as the Chicago Cyclotron Magnet. It has full solid angle coverage for tracking, Kaon and electron identification, and forward muon coverage.
6. The muon coverage for D0, the BSD, and the BCD is primarily in the forward regions, with requirements that $P > 3$ GeV/ c (to penetrate the hadron absorber) and $P_t > 1$ GeV/ c . It is assumed that CDF has only central muon coverage since the P_t trigger in the forward muon system has a threshold too high (5 GeV/ c) to affect the CP limits. We allow muons with $P > 2$ GeV/ c in the central region of CDF. The net advantage of the new detectors over CDF for muons is only a factor of a few. This advantage is available in a solenoid geometry only if the proposed silicon vertex detector actually functions as the forward tracker as well, at considerably greater cost than a silicon vertex detector for the BCD. The silicon tracker is being proposed by D0.
7. The electron coverage of the BSD and the BCD is assumed to include all $P_t > 1$ GeV/ c , for both forward and central electrons. While such coverage would be very advantageous, it will be quite difficult to obtain this in practice. It could only be obtained in CDF or D0 with a major upgrade to their electron-identification systems.
8. The use of Kaons is for tagging the second B via the sign of the Kaon from the $b \rightarrow c \rightarrow s$ cascade decay. The Kaon tag is about five times as useful as the lepton tags. We presume the needed compact RICH counter could be built for all detectors.

We draw some overall conclusions that are supported by additional arguments in Sections 3 and 5 below:

- A 3-dimensional vertex detector, large-solid-angle low- P_t lepton coverage, and Kaon identification are critical to a CP -violation capability at the Tevatron.
- No Tevatron experiment has a reasonable chance at measuring CP violation without the advantage of a Kaon tag, which requires Kaon identification. This is the decisive justification for hadron identification. The Kaon tag will be based on partial reconstruction of the second B in the event, for which no mass constraints will be available to compensate for an absence of hadron identification.
- The higher event rates at a Bottom Solenoid Detector (BSD) or a Bottom Collider Detector (BCD) with a dipole magnet arise because of increased coverage at forward angles (to which a solenoid field is not well matched) and because of electron identification down to very low transverse momentum. Useful forward muon coverage in a solenoidal detector can only be obtained at the expense of building a silicon tracker rather than a vertex detector. Also, the electron-identification system of the BSD would be a major upgrade beyond those already proposed by either CDF or D0.

3 The Need for a 3-D Vertex Detector

Although fixed-target experiments all use vertex detectors that provide three-dimensional (3-D) measurements of track coordinates, existing vertex detectors for collider experiments are typically two dimensional (2-D). Certainly there is extra complexity in constructing a 3-D vertex detector to provide 4π solid-angle coverage at a collider. Here we review why a 3-D vertex detector is essential for a collider B -physics experiment.

We desire the complete reconstruction of B decays to all-charged final states with high efficiency. To do this in a high-multiplicity environment, the B -decay tracks must be isolated from the primary interaction vertex by the observation of the secondary vertex of the B . The average path length perpendicular to the beam before a B decays is $\approx c\tau = 360 \mu\text{m}$, noting that $\langle P_t \rangle \approx M_B$. Silicon vertex detectors typically have position resolution of $10 \mu\text{m}$, which leads to (transverse) vertex resolution of $\approx 20 \mu\text{m}$. While this seems small compared to the typical path length of $360 \mu\text{m}$ that must be resolved, such a silicon vertex detector does not have excess capability, as discussed below.

In addition, we desire to study the mixing of the neutral B mesons, both for its own interest and as a necessity for the analysis of CP -violating decay asymmetries. This requires the determination of the proper decay time to a small fraction of the B lifetime. Again the (transverse) spatial resolution on the secondary decay vertex must be a small fraction of $c\tau = 360 \mu\text{m}$. Precision measurements, particularly important for B_s mixing, are clearly best made with a 3-D vertex detector.

In an experiment that does not aspire to study B_s mixing, could one deliver a viable signal of secondary B -decay vertices with a 2-D vertex detector? Note that two lines in 3-space are in general skew; they have a nonzero distance of closest approach. But in any 2-D projection those two lines appear to cross at some point. There is a qualitative loss of ability to distinguish three-dimensional secondary vertices from random track pairings by restricting measurements to two dimensions.

It is 'intuitively' plausible that if a 3-D vertex detector has a figure of merit F_{3D} for finding true secondary vertices, then a 2-D detector would have a figure of merit $F_{2D} \approx \sqrt{F_{3D}}$.

We illustrate this in a Monte Carlo simulation of events containing $B \rightarrow \pi^+\pi^-$ decays.^[2] In each event a search is first made for two-track (secondary) vertices consistent with the B mass. Then the remaining tracks are searched for the primary vertex. A measure of the significance of a secondary vertex is the ratio S/σ_S , where S is the distance between the primary and secondary vertices. A two-track secondary vertex will be considered physical only when $S/\sigma_S \gtrsim 10$.

We define the *merit factor* F as the number of detected $B \rightarrow \pi^+\pi^-$ secondary vertices divided by the number of false two-track secondary vertices. The simulated results are shown in Fig. 1. For a cut of $S/\sigma_S = 10$ we found that $F_{3D} \approx 24$, while the three different figures of merit for 2-D detectors were $F_{xz} \approx F_{yz} \approx 7$, and $F_{xy} \approx 3$. For a 2-D detector, the stripes of the silicon wafers are along the axis perpendicular to the measurement plane. Thus, the CDF vertex detector with its stripes along the z axis corresponds to F_{xy} .

While our simulation demonstrates the superiority of a 3-D vertex detector it does not yet prove that even this is adequate for a 'difficult' mode like $B \rightarrow \pi^+\pi^-$.

Our Monte Carlo simulation is consistent with the experience of the E-687 group. When reconstructing the three-body charm decay $D \rightarrow K\pi\pi$, they find a figure of merit of 300 for

Merit factor vs detachment significance for 3D and 2D algorithms

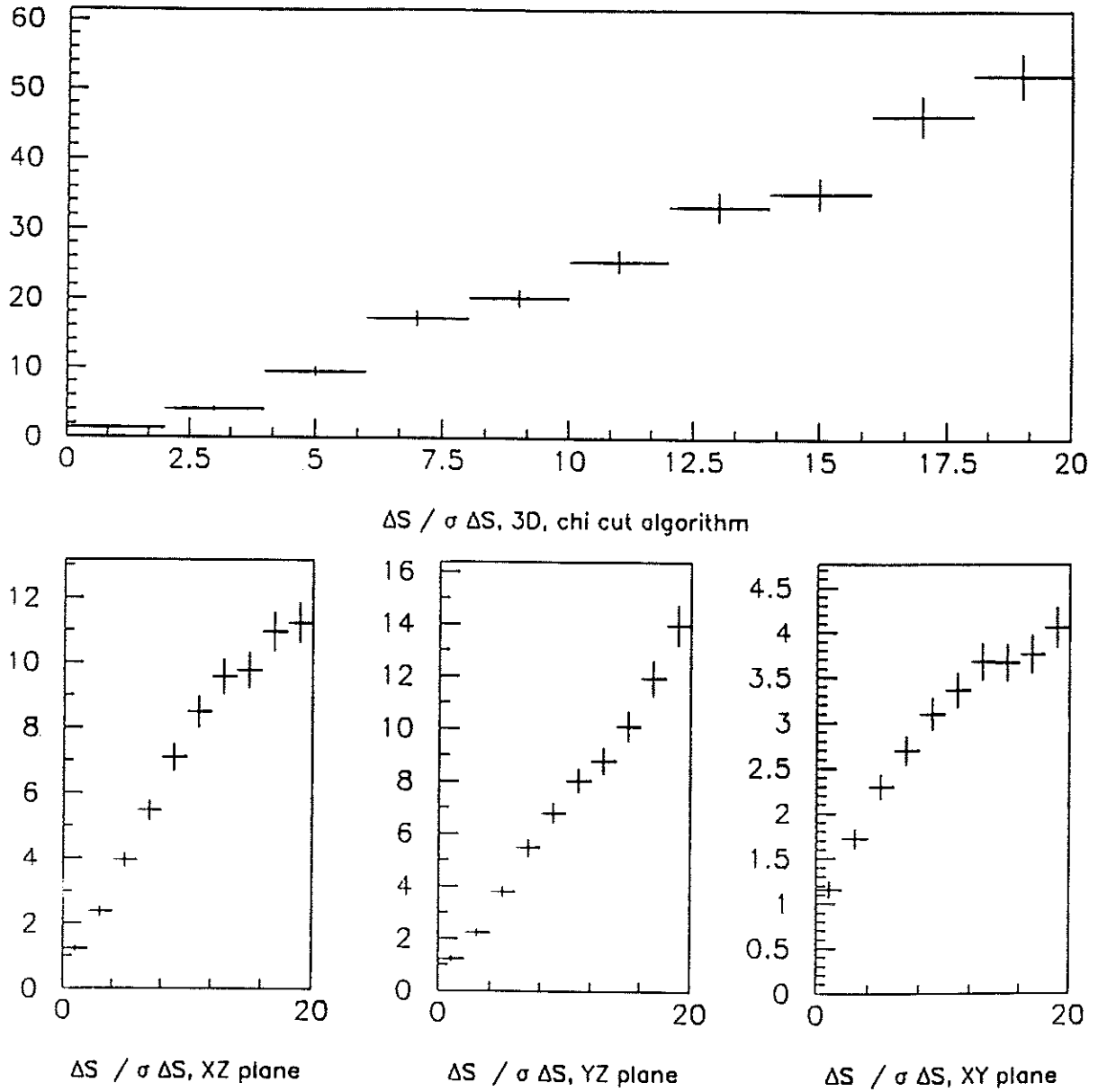


Figure 1: Figures of merit for 3-D (top) and 2-D (bottom) vertex detectors. The figure of merit is the number of correctly identified $B \rightarrow \pi^+\pi^-$ vertices divided by the number of false two-track secondary vertices in simulated events each containing a $B \rightarrow \pi\pi$ decay. S is the distance between the primary and secondary vertices.

a cut of $S/\sigma_S = 3.5$ using their 3-D vertex detector. The E-687 group has estimated that the figure of merit would be only ≈ 30 if a 2-D vertex detector had been used.

In an experiment that emphasizes study of $B \rightarrow J/\psi X$, the vertex detector would be less critical in identifying such decays as in identifying tracks belonging to the second, tagging B in the event. In general the decay products of the latter will include neutrals and the reconstruction will be partial. We must reliably isolate the charged decay products of the second B from the primary vertex to tag it as a particle or antiparticle. For this a simulated figure of merit of only a few, as for measurement in the x - y plane, is clearly untenable.

4 Vertex Detector R&D

A 3-D vertex detector with large solid-angle coverage has been argued in the previous section to be essential for an ambitious B -physics program at the Tevatron. The critical design features of such a detector are the mechanical alignment, which must be stable to a few microns over a meter, and the cooling, removing about two kilowatts of power from inside the detector.

The BCD is the only group undertaking R&D in these areas at Fermilab. Over the last two years we have constructed and tested a full-scale mechanical/thermal model of the silicon-vertex-detector support structure.^[3, 4, 5, 6] In addition, studies were made of the properties of glues, of tensile strengths of pyrex joints, and of cable prototypes. Work on the development of a new VLSI silicon-detector readout chip, and on evaluations of silicon detectors in test beams has been described elsewhere.^[7, 8, 9] Here we discuss progress since the last PAC meeting and present new requests in light of this progress.

An opportunity has arisen that will allow us to expand and improve our mechanical R&D program substantially. We are very fortunate to have begun the process of transferring a surplus ANORAD Coordinate Measurement Machine (CMM) from MIT to Fermilab. Though not yet in hand, we are optimistic this machine will be available for use by the BCD within the next two months. The CMM is being purchased by the Fermilab Physics Department for only a few thousand dollars, compared to its original price of about \$100k. The machine will be located in Lab 7, and the Fermilab Physics Department is making a strong effort to supply the technician to operate it. We have outlined in Ref. [6] how such a machine could be modified for precision assembly of a 3-D silicon vertex detector.

The CMM will play a central role in our next generation of vertex detector R&D. The mechanical studies fall into four major categories:

1. The study of single silicon-detector wafers can be divided into four subcategories.
 - (a) First the study of adhesives, though well underway, is not yet complete. The glues used to adhere the readout chips to the wafers must be shown to be insensitive to both neutron and gamma radiation.
 - (b) Second, it is not known whether the glues will react chemically with the surface of either single- or double-sided detectors or AC-coupled detectors, the latter having more extensive surface dopings. We have proposed tests that monitor the pulse-height spectrum from a radioactive source before and after the glues are presented to the detector surfaces.

- (c) The third area of concern is the large amount of local heating from the BVX readout-amplifier chips^[7] that are glued directly to the silicon-detector wafer. A measure of the noise performance of the BVX *in situ* is very important.
 - (d) Finally, the readout-cable design will be tested by attaching prototype cables to the wafers and studying the effect of heat flow on the mechanical rigidity. Cable termination on the silicon wafer is yet to be developed. Funds needed for substrate and termination-plate samples and contract bonding total \$8k.
2. The study of multi-wafer assemblies, called modules, requires an assembly procedure with associated fixtures. This work would not be done with the CMM. The purpose of assembling a module is to study the breakage properties of the silicon during assembly and in routine handling of a module.
- (a) The assembly fixtures have been designed but not yet built. The fixtures need to be tested and new ones made if the first pass indicates the results are not adequate. Funds of \$15k are required for this.
 - (b) We have on hand most of the raw materials needed to construct two modules of custom-cut 'junk' silicon using ultraviolet-cured glue and small glass prisms to provide mechanical bridges between wafers. The procedures are detailed in Ref. [6], and we could build such a module in two months. The quoted cost by industry of cutting the glass prisms is between \$10k and \$15k dollars. We have decided to make prototype prisms ourselves and at a cost of \$6k.
 - (c) After the module is constructed, we would perform stress tests on the wafers and joints, tests of creep *vs.* temperature and radiation dosage. It is also important to determine with what accuracy we can measure the placement of the individual wafers. An inspection pedestal has been designed for this purpose but not yet built. Funds needed for the inspection pedestal are \$3k.
 - (d) We hope to be able to disassemble the module with a solvent. This would be very useful in an operating system since it would facilitate repairs to the detector. We are exploring the use of various adhesives that can later be dissolved, but have yet to test the full procedure.
 - (e) Finally, a major issue is the cable routing from inner layers to outer layers. Cables are sources of electrical pickup, multiple coulomb scattering, and impedance to cooling-air flow. The importance of a careful cable-plant design cannot be overemphasized. In our present design we have openings at various locations in the module. We have tested cabling methods using paper cables on a plastic model, but no real cable test on a silicon module has been performed.
3. The assembly studied in item 2 will be by hand, and so has limited accuracy and would not be suitable for a large vertex detector. The ANORAD Coordinate Measurement Machine allows us to address assembly techniques at the accuracy needed for the final vertex detector. We must first upgrade the CMM with features relevant to assembling precision silicon structures: A video camera (+ monitor and video printer), a vacuum-based robotic attachment for prism/wafer placement, and a PC with control software.

Funds of \$64k are needed for this. We estimate that an initial 3-D silicon assembly could be completed within six months. People to perform this work have already been identified.

4. During the last two years we performed tests on a 3-meter model of the silicon-vertex-detector support tube ('gutter').^[3, 4, 5] The gutter doubles as the mechanical support for a silicon detector that is long (i.e., detects particles in the forward rapidity range as well as central) and is the conduit to which cooling is applied. This mechanical model has already provided many results and continuing this work is very important. An upgrade of the full-scale test station is necessary for more precise results from thermal and vibrational measurements. A new location for the tests that includes an environmentally controlled room has been found at the lab. An engineering physicist is needed who can spend 50% time on this project. In addition, we estimate that \$30k is needed to purchase position sensors that provide accuracies down to a micron, a new blower for improved cooling, and a better liquid-cooling assembly.

In summary, the mechanical tests are as critical to the success of a next-generation vertex detector as the readout chips are to this generation of detectors. We emphasize that progress in all four categories are needed in the next year before a full system design can be attempted. The acquisition of the CMM and its full exploitation is critical for the success of this program. We seek funds of \$126k and an engineering physicist 50% time are needed to make major progress in the next 9 months, as summarized in Table 2.

Table 2: Funding request for continued R&D on a 3-D silicon vertex detector.
We also seek a half-time engineering physicist to work on this project.

1. Readout-cable prototypes.....	\$8k
2. Multi-wafer assembly fixtures (non-robotic).....	\$15k
3. Glass prisms	\$6k
4. Inspection pedestal.....	\$3k
5. Multi-wafer assembly fixtures (robotic)	\$64k
6. Upgrade of full-scale test station.....	\$30k
7. Total.....	\$126k

5 The Need for Kaon Identification

There are two important reasons for Kaon identification in a B -physics experiment:

1. The most effective tag as to the particle/antiparticle character of a neutral B is via the sign of the Kaon from a $b \rightarrow c \rightarrow s$ cascade decay of the second B in the event. This is needed for studies of CP violation as well as for B - \bar{B} mixing.
2. The majority of all-charged decays of B and D mesons include one or more Kaons.

Of these, the first reason is the critical one. Without Kaon identification there is very little prospect of accumulating a large enough sample of tagged B decays at the Tevatron to study CP violation.

When reconstructing an all-charged decay of a B or D meson, mass constraints may provide sufficient ability to identify Kaons in software without a hardware device for that purpose.

These issues are discussed in greater detail in the following two subsections.

5.1 Efficiency of Lepton and Kaon Tags

[This subsection appeared as Sec. 7.5 of Ref. [1], but we repeat it here to give it further emphasis.]

In this section we argue that a Kaon tag (which requires Kaon identification) would be about five times as effective as combined electron and muon tags.

We propose to determine the particle/antiparticle character of a fully reconstructed B meson via a tag on the second B in the event. The tag would be based on the sign of the lepton in a partial reconstruction of the decays $B \rightarrow l^\pm X$, or on the sign of the Kaon in $B \rightarrow K^\pm Y$. The lepton tag would be available for at most 20% of the events (due to the semileptonic branching fraction). Kaons occur in almost 100% of all B decays via the cascade $b \rightarrow c \rightarrow s$. Charged Kaons occur in about 65% of all B decays, taking into account Kaons arising from the decay of virtual W bosons associated with the quark-flavor transitions.

For all tags there is some probability of mistagging from a wrong-sign lepton or Kaon due to secondary and tertiary decays. If the probability is p that a wrong-sign tag is made, then the statistical power of a sample of N tagged events is reduced to that of $N(1 - 2p)$ perfectly tagged events. We will find below that mistagging is more probable for the lepton than the Kaon tag, if one integrates over the entire transverse-momentum spectrum of the leptons and Kaons.

Since we only have to worry about the tagging quality when we have a fully reconstructed B , we can have confidence that any other secondary vertex in the event is that of the second B , even if the latter is only partially reconstructed. Hence we only examine the decays of the second B to estimate the mistagging probability p . For this we have generated a sample of 10^5 B - \bar{B} pairs at TEV I using ISAJET, and let them decay according to a representative sample of hadronic and semileptonic modes following Bjorken.^[10]

The P_t spectra of right-sign leptons (from the primary decay $b \rightarrow W^- \rightarrow l^- \nu$) and of wrong-sign leptons (from the secondary decay $b \rightarrow c \rightarrow W^+ \rightarrow l^+ \bar{\nu}$, etc.) are shown in Fig. 2. There are actually about 1.5 times as many wrong-sign leptons as right sign, although the

wrong-sign leptons have markedly lower P_t . The P_t spectrum of right-sign Kaons (from $b \rightarrow c \rightarrow s$ with the s -quark appearing in a Kaon) is shown in Fig. 3, and is essentially identical to that of wrong-sign Kaons (from $b \rightarrow W^- \rightarrow \bar{c} \rightarrow \bar{s}$, or $b \rightarrow c \rightarrow W^+ \rightarrow \bar{s}$, etc.). However, right-sign Kaons outnumber wrong-sign Kaons by 6 to 1 (according to the model branching fractions of Ref. [10]).

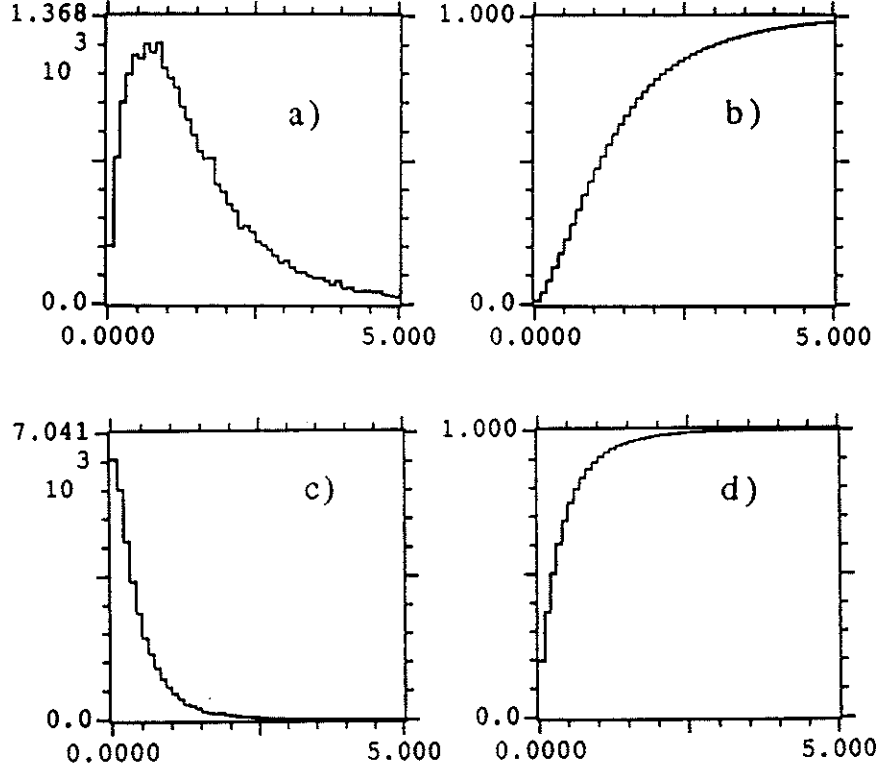


Figure 2: a) The P_t spectrum for single leptons from $B \rightarrow l^\pm X$. b) The integral spectrum of a). c) The P_t spectrum for leptons from $B \rightarrow DX$ with $D \rightarrow l^\pm Y$. d) The integral spectrum of c).

In using the leptons (or Kaons) to determine the particle/antiparticle character of the second B we simply look at the sign of the highest- P_t lepton (or Kaon). Only in a small fraction of the decays are there two leptons (or two Kaons) and we have made no attempt to devise a more sophisticated algorithm for this small subset.

Figure 4 shows the fraction of all leptons (or Kaons) at a given P_t that have the wrong sign. While at no P_t are wrong-sign Kaons a problem, for $P_t < 500$ MeV/c the wrong-sign leptons dominate the right-sign. That is, the lepton tag is worthless at $P_t = 500$ MeV/c. For P_t less than this we can change our definition of 'right' and 'wrong' and obtain some useful tags.

The effectiveness of the tags is presented another way in Fig. 5. The quantity $N|1 - 2p|$, the effective number of useful events, is plotted as a function of P_t in the left-hand plots.

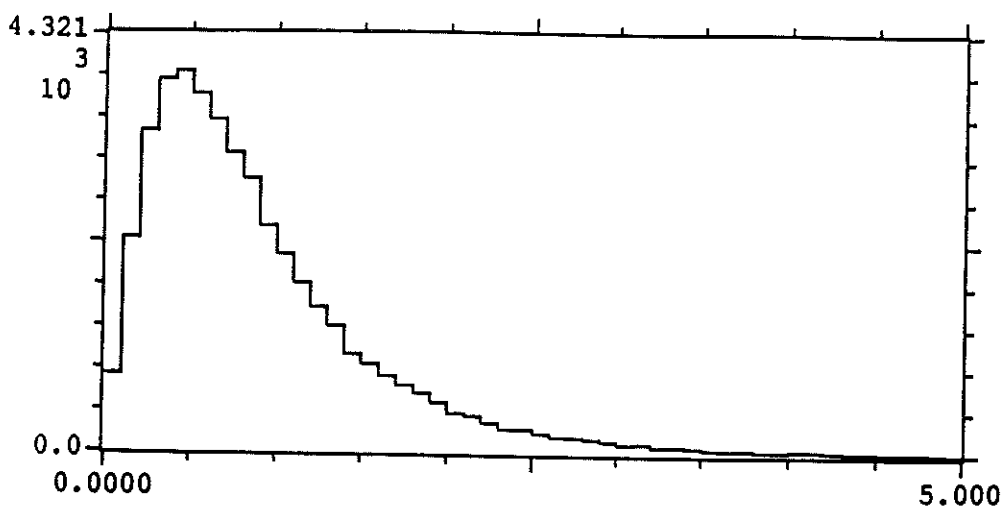


Figure 3: The transverse-momentum spectrum of right-sign Kaons from B -meson decay.

The right-hand plots show the integral

$$\int_{P_t}^{\infty} dN |1 - 2p|.$$

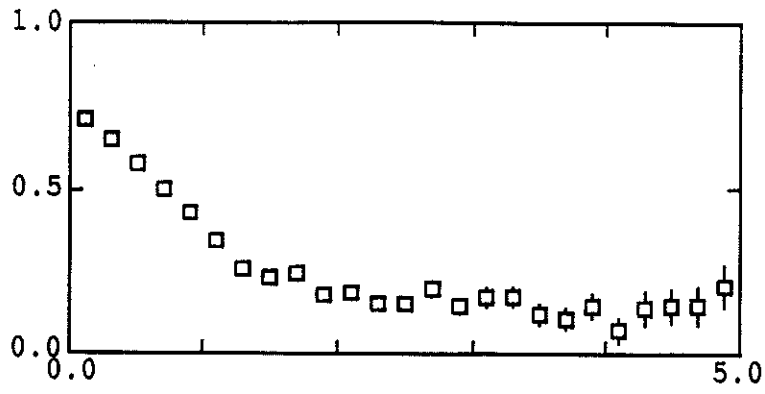
The integrals have been normalized to the total number of B 's, and so represent the efficiency of a tag as a function of the minimum- P_t cut.

The Kaon tag will be about 10 times as useful as a lepton tag, or 5 times as useful as the combination of electron and muon tags.

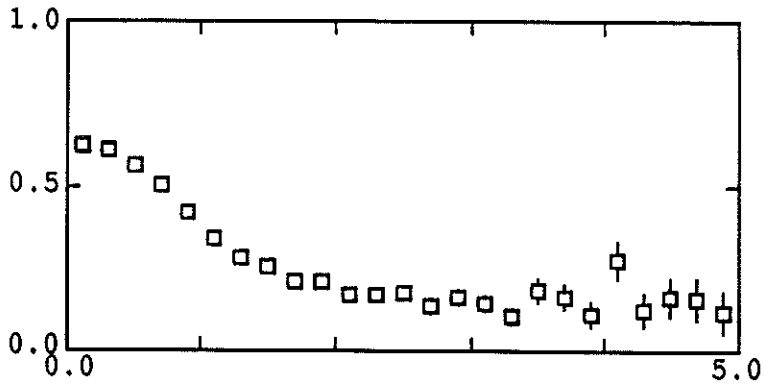
The efficiency of the lepton tags increases only slightly as the P_t cut is lowered below 1 GeV/c, due to the abundance of low- P_t wrong-sign leptons. A way around this is to use a combined lepton and Kaon tag, requiring both a right-sign lepton and Kaon. Row three of Fig. 5 shows how for very low P_t this tag becomes more efficient than a lepton tag alone, although at high P_t it is only 1/2 as efficient. The combined lepton and Kaon tag is superior from the point of view of immunity to backgrounds we have not considered here.

5.2 Kaon Identification Via Mass Constraints

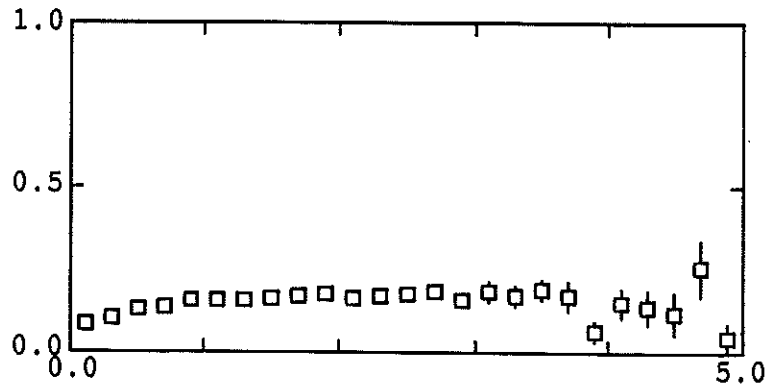
In this section we show that if the B -decay products have been successfully isolated from the rest of the event (by a vertex detector) then all-charged modes can be reconstructed correctly with good probability without hardware particle identification. However, misidentifications of decays with neutrals, and confusions between the B_d and B_s , are shown to be so severe that particle identification is warranted. Of course, there is extensive experience in the community that particle identification is vital when background tracks are present in the sample.



wrong sign e fraction vs PT



wrong sign mu fraction vs PT



wrong sign K fraction vs PT

Figure 4: The fraction of leptons (or Kaons) that have the wrong sign as a function of P_t .

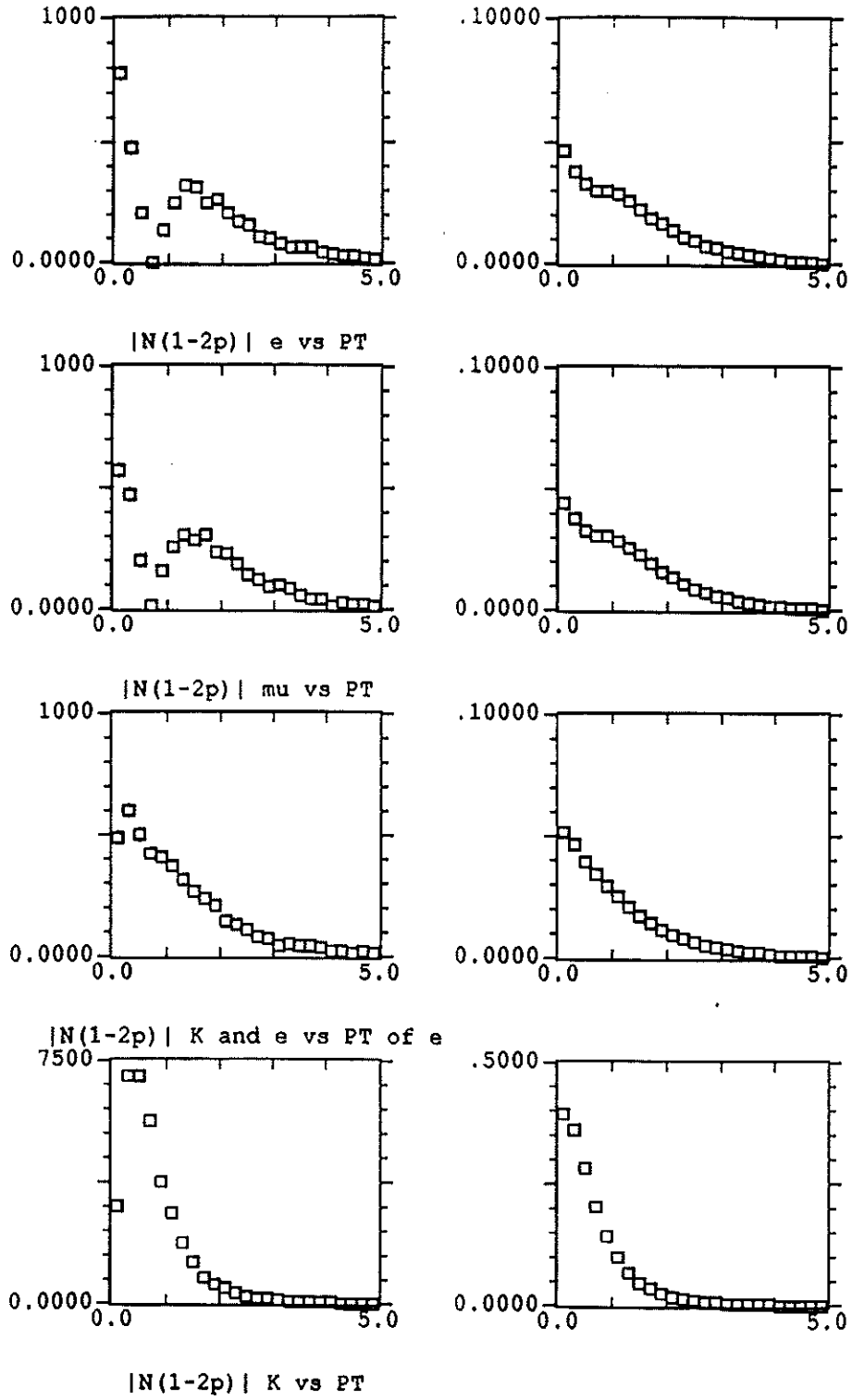


Figure 5: Differential and Integral tagging efficiencies of four types of tags as a function of transverse momentum. Left hand plots: the number $N|1 - 2p|$ of useful tagged events; right-hand plots: the total efficiency of the tag as a function of the minimum-transverse-momentum requirement. The four tags are, from top to bottom, electron, muon, combined electron and Kaon, and Kaon.

For our study we used the sample of 10^5 $B\bar{B}$ pairs generated by ISAJET as described in the previous subsection. We suppose that the accuracy of the momentum measurement of the charged tracks is

$$\frac{\sigma_P}{P} = \sqrt{(0.004)^2 + (0.0015P_t)^2}.$$

This is a good approximation to the resolution currently achieved in CDF, and reproduces their mass resolution of 17 MeV/ c^2 for $J/\psi \rightarrow \mu^+\mu^-$ decays with $P_t > 2$ GeV/ c for the muons, and $P_t > 4$ GeV/ c for the J/ψ .

We begin with the charged meson B_u . Among the sample of 10^5 B decays were 133 examples of $B_u \rightarrow$ all-charged tracks. In the absence of hadron identification we supposed that each track could be either a pion or a Kaon. For an n -body decay there are then 2^n different hypotheses as to the identity of the tracks. For each of these we calculated the invariant mass, using track momenta smeared according to the above prescription.

- The hypothesis with reconstructed mass closest to the known mass of the B_u was taken as the ‘correct’ one.

In 76% of the cases this analysis actually provided the proper particle identification. Some details are given in Table 3. At this stage we ignore the possibility that the decay includes separated vertices due to cascade D - or K -meson decays.

Table 3: The numbers of $B_u \rightarrow$ all-charged decays for which the correct particle identification was obtained by examining which hypothesis yielded the best invariant mass. Also shown are the numbers of correct identifications when the ‘plausibility’ cut, described in the text, is applied as well.

n_{track}	Correct ID Via Best Mass	Plausibility Cut	Total Events
3	3	1	4
5	12	2	21
7	25	11	38
9	33	18	38
11	23	14	27
13	5	4	5
all	101	50	133

The results of Table 3 are very encouraging, but they were obtained with the knowledge that the set of tracks to be studied was the proper one. In practice we will not have this knowledge. For example, most B decays contains neutrals that cannot be associated with the charged tracks by the vertex detector. Most likely we will have to consider the neutrals as missing. The remaining charged tracks that fit to a secondary vertex are then

(incorrectly) presented as candidates for an all-charged decay of the B . With the correct particle identification of these tracks, their combined invariant mass would be less than the B mass by at least M_π and the event could be rejected. However, without particle identification, hypotheses in which pions are called Kaons lead to larger invariant masses and might by accident coincide with the B mass.

In an attempt to reject track sets with missing neutrals we make an additional requirement:

- The hypothesis with invariant mass closest to the B mass is considered valid only if the mass difference is less than two standard deviations.

From the known form of the momentum resolution the error on the invariant mass of a given track set can be estimated for this. With momentum resolution as given above the B -mass resolution is rather good, varying from 17 MeV/ c^2 for 3-track decays to only 7 MeV/ c^2 for 13-track decays.

However, even using our revised prescription a large number of B_u decays with missing neutrals were claimed to be correctly identified all-charged decays. The numbers of events are summarized in Table 4. In particular we see that events with large numbers of charged tracks are readily misidentified.

Table 4: The numbers of B_u decays with missing neutrals for which an hypothesis as to the identity of the charged tracks led to an all-charged invariant mass within $\pm 2\sigma$ of the B mass. These events would then be incorrectly identified. Also shown are the numbers of decays with missing neutrals that pass the ‘plausibility’ cut.

n_{track} (charged)	‘Correct’ ID Via 2- σ Cut	Plausibility Cut	Total Events
3	4	1	2982
5	268	114	5512
7	1448	338	5560
9	2786	161	3497
11	1252	9	1266
13	235	3	237
all	5993	626	19054

On examining the decays with missing neutrals that were mistakenly identified as all-charged decays, we noticed that if an event is misidentified there are often many different ways of doing this all with invariant-mass hypothesis close to the true B mass. On the other hand, in the true all-charged decays typically only the correct particle identification led to a mass close to the B mass. Accordingly we have applied an additional criterion for particle identification:

- When N different hypotheses as to the identity of the charged tracks all lead to invariant masses within $\pm 2\sigma$ of the B mass, we define the ‘plausibility’ of the identification as $1/N$. Only decays with plausibility $> 90\%$ are considered to be identified.

The use of the ‘plausibility’ cut significantly reduces the number of events with missing neutrals that are mistakenly identified as all-charged decays, as also summarized in Table 4. The effect of applying the plausibility cut to the true all-charged decays is shown in Table 3, where we see that 38% of the all-charged events survive the plausibility cut. Unfortunately, because there are so many more decays with neutrals than all-charged tracks, the number of misidentified decays that pass our cuts is still larger by an order of magnitude than the number of correctly identified all-charged decays.

Thus far we have not taken advantage of the possibility that some of the B -decay products arise from the tertiary decay of a long-lived D or K meson. With a vertex detector that correctly associates these tracks with a separated vertex, additional constraints will be available. Here we estimate the maximum advantage that might be obtained from tertiary vertices by examining the decays $B_u \rightarrow D^0 + \text{all-charged tracks}$.

We suppose that the D^0 is correctly identified in a separate study, and all that remains is to identify the charged tracks associated with the B -decay vertex. Again we examine the invariant masses of the various particle-ID hypotheses and apply the plausibility cut, with results as shown in Table 5. The tertiary vertex can indeed be very helpful; in contrast to the results of Table 3, we now correctly identify 94% of the B_u decays. Of course, one must factor in the probability that the tertiary vertex is correctly analyzed.

Table 5: The numbers of $B_u \rightarrow D^0 + \text{all-charged decays}$ for which the correct particle identification was obtained by examining which hypothesis yielded the best invariant mass. Here the D^0 has been assumed to have been correctly identified via its decay products which form a separated tertiary vertex.

n_{track} (charged)	Correct ID Via 2- σ Cut	Plausibility Cut	Total Events
2	25	18	25
4	22	20	23
6	35	35	35
8	11	11	12
10	2	2	3
all	95	86	98

We must also consider those events in which a D^0 is successfully reconstructed at a tertiary vertex, but the tracks from secondary B vertex include neutrals. According to Ref. [10] the situation here is relatively favorable in that a substantial fraction of the decays $B_u \rightarrow D^0 X$ have X as all-charged. The results of our simulation are shown in Table 6, where

we infer that the observation of a tertiary D vertex could raise the signal-to-noise to 2 : 3. However, we would still prefer a signal-to-noise much larger than one.

Table 6: The numbers of $B_u \rightarrow D^0 + X$ decays where X includes missing neutrals for which the charged tracks were incorrectly identified as reconstructing to the B mass. The D^0 has been assumed to have been correctly identified via its decay products which form a separated tertiary vertex.

n_{track} (charged)	'Correct' ID Via		Total Events
	2- σ Cut	Plausibility Cut	
2	24	17	298
4	33	29	261
6	79	64	236
8	50	24	75
10	8	4	9
all	194	138	879

We now turn to the neutral mesons, B_d and B_s . These have masses that differ by only a small amount (the value is not presently known, but was taken as 200 MeV/ c^2 in this study). If we have a set of tracks whose total charge is zero associated with a secondary vertex, then we must compare our hypotheses as to the particle ID's with both the B_d and the B_s . We might well have a B_d mistakenly identified as a B_s , or *vice versa*. A measure of the probability of this is given in Tables 7 and 8.

With two mass hypotheses to be considered for each neutral decay, there are typically so many ways of satisfying one or the other hypothesis that our 'plausibility' cut is of little use. The problem of B_d 's being misidentified as B_s 's is particularly severe as there will be many more all-charged decays of the B_d than of the B_s .

We have attempted to derive an advantage from the existence of tertiary decays in another manner. The B -decay products may include daughter mesons such as D , J/ψ , ϕ , K_S ... that decay in turn. This time we do not suppose that the daughters have separated tertiary vertices, but that their decay products are intermixed with those directly from the B decay. However, we examine subsets of the B -decay tracks for those that reconstruct to the mass of one of the possible daughter mesons. This search is more fruitful if we restrict ourselves to hypotheses for the decay products of the daughters that lead to a B mass when combined with the rest of the tracks from the B decay. Tables 9 and 10 list the fraction of all-charged B_d decays that are thus correctly reconstructed in this manner, and the numbers of misidentified decays when there are missing neutrals. With this approach we only achieve a signal-to-noise of 1 : 4.

While our present study does not exhaust the possibilities of analyses of B decays without explicit particle identification, it indicates that the signal quality will not be high. In view

Table 7: The numbers of $B_d \rightarrow$ all-charged decays for which the correct particle identification was obtained by examining which hypothesis yielded the best invariant mass. Also listed are the numbers of decays for which the ‘best’ particle-ID hypothesis fitted to the B_s mass.

n_{track}	Correct ID as B_d	Wrong ID as B_s	Total Events
4	169	33	222
6	48	44	105
8	35	40	87
10	23	17	43
12	8	6	15
all	283	140	472

Table 8: The numbers of $B_s \rightarrow$ all-charged decays for which the correct particle identification was obtained by examining which hypothesis yielded the best invariant mass. Also listed are the numbers of decays for which the ‘best’ particle-ID hypothesis fitted to the B_d mass. The ‘plausibility’ cut has been applied.

n_{track}	Correct ID as B_s	Wrong ID as B_d	Total Events
4	8	2	11
6	19	2	25
8	17	2	23
10	2	2	4
12	4	2	7
all	50	9	70

of this it appears wise to provide for Kaon identification in the hardware.

Table 9: The numbers of $B_d \rightarrow$ all-charged decays for which the correct particle identification was obtained by simultaneous fits for the B mass and the mass of a daughter meson. No use is made of a possible tertiary vertex. The column labelled ‘ $2\text{-}\sigma$ Cut’ includes all decays for which the correct particle identification leads to B and daughter masses both within 2σ of the true value, whether or not this identification was the ‘best.’

$n_{\text{daughters}}$	Correct ID Via		Total
	$2\text{-}\sigma$ Cut	Plausibility Cut	Events
2	47	32	47
3	153	112	181
4	162	132	189
5	47	32	65
6	28	12	47
7	18	12	41
8	9	4	29
9	12	9	21
10	6	1	17
11	5	4	6
12	2	0	3
13	2	1	2
all	491	351	648

Table 10: The numbers of $B_d \rightarrow X$ decays for which X includes missing neutrals and an incorrect particle identification was obtained by a simultaneous fit for both the B mass and the mass of a daughter meson.

n_{track} (charged)	'Correct' ID Via 2- σ Plausibility Cut		Total Events
2	3	3	2014
3	14	10	1257
4	196	86	9383
5	366	177	2553
6	2034	563	9565
7	1006	272	2421
8	3248	319	5583
9	791	53	1005
10	850	29	976
11	182	4	186
12	113	0	116
13	19	0	21
all	8822	1516	35080

6 Comments on CP -Violation Physics

In this section we make a number of brief comments to supplement the lengthier discussions of the physics of CP violation we have given elsewhere.^[1, 11]

6.1 The Four Classes of CP Violation of Neutral B Mesons

CP violation can be very prominent in the B -meson system because the relevant CP -violating phases in the CKM matrix occur in first order. This is in contrast to the K -meson system where CP -violating phases arise in the relevant matrix elements only in higher order.

In the neutral B -meson system there are four classes of CP violation, as readily seen in the Wolfenstein representation of the CKM matrix. For this we need only note the location of the matrix elements that have imaginary parts (to first order):

$$V_{CKM} = \begin{pmatrix} V_{ud} & V_{us} & V_{ub} \\ V_{cd} & V_{cs} & V_{cb} \\ V_{td} & V_{ts} & V_{tb} \end{pmatrix} \approx \begin{pmatrix} \text{Re} & \text{Re} & \text{Im} \\ \text{Re} & \text{Re} & \text{Re} \\ \text{Im} & \text{Re} & \text{Re} \end{pmatrix}.$$

The phase of V_{td} enters in B_d (but not B_s) mixing due to top-quark exchange in the box diagram.

The phase of V_{ub} enters in $b \rightarrow u$ (but not $b \rightarrow c$) decays.

Hence there are 4 classes of CP violation in decays of neutral B 's, as listed in Table 11.

Table 11: The four classes of CP violation in the neutral B -meson system.^[12]

Class	Parent	Quark Transition	Example	CP -Violating Phase
1	B_d	$b \rightarrow c$	$B_d \rightarrow J/\psi K_S$	$\varphi_1 = \varphi(V_{td})$
2	B_d	$b \rightarrow u$	$B_d \rightarrow \pi^+ \pi^-$	$\varphi_2 = \varphi(V_{td}) + \varphi(V_{ub})$
3	B_s	$b \rightarrow u$	$B_s \rightarrow \rho K_S$	$\varphi_3 = \varphi(V_{ub})$
4	B_s	$b \rightarrow c$	$B_s \rightarrow J/\psi \phi$	$\varphi_4 = 0$

For decays of neutral B 's to CP eigenstates f , the observable effect is the decay asymmetry

$$A(t) = \frac{\Gamma(B \rightarrow f) - \Gamma(\bar{B} \rightarrow \bar{f})}{\Gamma(B \rightarrow f) + \Gamma(\bar{B} \rightarrow \bar{f})} = \sin 2\varphi_i \sin xt,$$

where φ_i is the relevant phase of the CKM matrix element listed above, $x = \Delta M/\Gamma$ is the mixing parameter, and t is the proper time of the decay.

As there are three classes of nonzero asymmetries, we can make three measurements of the two CKM phases, and hence overconstrain the Standard Model.

This insight is also commonly expressed via the unitarity triangle. But it is important to note that the Standard Model predicts a null effect in a fourth class of decays, which are quite accessible at the Tevatron.

6.2 The Einstein-Rosen-Podolsky Effect

If the $B^0\text{-}\bar{B}^0$ pair is produced in a $C(\text{odd})$ or $C(\text{even})$ combination, this quantum-mechanical correlation is maintained until both B 's decay, even though they may be spatially separated, and they decay at different times. The complexity of such correlations was first noticed by Einstein, Rosen, and Podolsky^[13] in a famous paper in which they argued that this indicates that quantum mechanics is an incomplete theory. However, no one seriously doubts that the EPR effect is real.

The application of the EPR effect to the neutral B -meson system was first noted by Carter and Sanda.^[14] Suppose that one B meson (B_1) decays to a CP eigenstate f at time t_1 , and that the second B meson (B_2) decays at time t_2 to a state $g \neq \bar{g}$ (such as $B \rightarrow l^\pm \nu X$) that allows us to determine whether it was a B or \bar{B} at time t_2 . Then the combined decay asymmetry

$$A(t_1, t_2) = \frac{\Gamma(B_1 \rightarrow f)\Gamma(\bar{B}_2 \rightarrow \bar{g}) - \Gamma(B_1 \rightarrow f)\Gamma(B_2 \rightarrow g)}{\Gamma(B_1 \rightarrow f)\Gamma(\bar{B}_2 \rightarrow \bar{g}) + \Gamma(B_1 \rightarrow f)\Gamma(B_2 \rightarrow g)} = \sin 2\varphi \sin(x_1 t_1 \mp x_2 t_2),$$

where the minus sign holds for $C(\text{odd})$ states: $|B_1 \bar{B}_2\rangle - |\bar{B}_1 B_2\rangle$.

If we don't observe the decay times, the integrated asymmetry is

$$A = \frac{x_1 \mp x_2}{(1 + x_1^2)(1 + x_2^2)} \sin 2\varphi,$$

which vanishes for $C(\text{odd})$ states in which $B_1 = B_2$ (i.e., $B_d \bar{B}_d$ or $B_s \bar{B}_s$).

For $B_d^0\text{-}\bar{B}_d^0$ produced at the $\Upsilon(4S)$ at an e^+e^- collider, we have only $C(\text{odd})$ states, and hence there will be no signal for CP violation unless one can observe the time evolution. This is the well-known justification for the construction of an asymmetric e^+e^- collider, which would be a costly consequence of the EPR effect.

6.3 Dilutions Due to Mixing

We continue the theme of the previous subsection by considering the case of a hadron collider (at c.m. energies far above B -production threshold). Here, $B^0\text{-}\bar{B}^0$ pairs are produced as incoherent sums of $C(\text{odd})$ and $C(\text{even})$ states. Then we see from the above that the combined decay asymmetry averages to

$$A(t_1, t_2) = \sin 2\varphi \sin x_1 t_1 \sin x_2 t_2,$$

and the integrated asymmetry averages to

$$A = \frac{x_1}{1 + x_1^2} \frac{1}{1 + x_2^2} \sin 2\varphi.$$

That is, the effects of the time dependences of the decays of the first and second B 's factorize, and the result is the same as if we had not concerned ourselves with the EPR effect at all.

However, this analysis emphasizes another important point: the 'dilutions' due to mixing if one makes time-integrated measurements. This refers to the factors $x_1/(1 + x_1^2)$ and

$1/(1+x_2^2)$ that multiply $\sin 2\varphi$ in the asymmetry. They arise because of the uncertainty that a neutral B meson has the same particle/antiparticle character at production and decay.

When $x_1 \lesssim 1$, as for the B_d , there are several lifetimes per period of oscillation, so even a time-resolved study of the decay is little different from a time-integrated study. Hence the measurable asymmetry of B_d decays will always be subject to a factor $\approx x_d/(1+x_d^2) \approx 0.5$, using the current experimental value that $x_d = 0.7 \pm 0.1$.

For B_s decays where $x_s \gg 1$ we have shown in Sec. 3.3.2 of Ref. [1] that the appropriate dilution factor (for meson 1) is $2/\pi$, assuming a time-resolved analysis.

In addition, there is a second dilution factor, $1/(1+x_2^2)$, due to mixing of the second, tagging B . The second dilution factor differs from the first because the final state $g \neq \bar{g}$ for the second B meson, while the final state $f = \bar{f}$ for the first meson. The second dilution factor was deduced from a different argument in Sec. 3.2.2 of Ref. [1].

At a hadron collider the second B can be a B_u , a B_d , or a B_s . The B_u does not mix ($x_u = 0$), so has a dilution factor we can call 1, the B_d has a dilution factor $\approx 2/3$, while the B_s has a dilution factor ≈ 0 if $x_s \gg 1$ as expected. Supposing the three flavors of B mesons are produced in the ratios $B_u : B_d : B_s = 0.375 : 0.375 : 0.25$, the overall dilution factor for the second meson would be 0.63. Allowing for the possibility of misidentifying whether the second B is a particle or antiparticle, we take the second dilution factor to be ≈ 0.5 . (It is convenient to remember both the first and second dilution factors as 0.5, but the detailed reasoning differs considerably.)

B_s mesons are essentially useless for tagging unless they can be identified and the decay time measured. But the second, tagging B will likely be only partially reconstructed, which will not permit an evasion of the dilution due to mixing.

The second dilution due to mixing could be avoided by restricting the tag to B_u . However, only 35-40% of the second B 's will be B_u , so unless these can be definitely identified as such with greater than 60% efficiency there is no advantage over tagging without flavor identification of the second B .

We summarize this section by noting that the smallest value of $\sin 2\varphi$ in a CP -violating asymmetry that can be resolved to three standard deviations with N events is not $3/\sqrt{N}$ but rather

$$\sin 2\varphi_{\min, 3\sigma} \approx \frac{3 \cdot 2 \cdot 2}{\sqrt{N}} = \frac{12}{\sqrt{N}}$$

at a hadron collider. The two factors of 2 are the dilutions due to mixing of the first and second B 's. At an asymmetric e^+e^- collider the corresponding sensitivity would be $9/\sqrt{N}$.

6.4 The Superweak Model

The superweak model is often used as a vehicle for discussions of alternatives to the Standard Model of CP violation. The comments below are based on conversations with B. Winstein and L. Wolfenstein.^[18]

The superweak model is that CP -violating effects are due to a new interaction that manifests itself only in the mixing of a neutral meson and its antiparticle. The effect is small, but different for each type of neutral meson. In the superweak model there are only two classes of CP violation in the neutral B mesons, one for B_d , and another for B_s . This

contrasts with the four classes discussed above in the Standard Model. Thus the observation that either

1. $\sin 2\varphi_1 \neq \sin 2\varphi_2$, or that
2. $\sin 2\varphi_3 \neq \sin 2\varphi_4$

would contradict the superweak model. In the Standard Model it is possible that $\sin 2\varphi_1 = \sin 2\varphi_2$, but it is extremely unlikely that both equalities would hold simultaneously.

A third confrontation between the superweak and Standard Models is possible with B mesons:

3. The Standard Model suggests that there will be small but nonzero CP -violating asymmetries in the decay rates of B^+ and B^- mesons, while the superweak model predicts a null effect.

7 Concluding Remarks

We conclude with a few remarks and a reiteration of the goal of the μ BCD.

1. B physics should be pursued as a **program** of study at Fermilab and not simply a subtopic of a high- P_t collider detector.
2. A B -physics experiment that seeks to study CP violation must include the following three technologies: a 3-D large-solid-angle silicon vertex detector, Kaon identification, and a high-rate data-acquisition system.
3. The BCD Collaboration has made substantial progress in all these areas with very limited resources.
4. We encourage the PAC and Fermilab to expand and improve upon the start of BCD towards a collider B -physics experiment at Fermilab by forming an in-house group dedicated to this research.
5. The μ BCD concept, an R&D program followed by physics studies, will focus interested parties on B physics in the next 5 years.
6. The experience gained from developing the stated technologies and the observation of B_s mixing is the best way for Fermilab to compete with e^+e^- proposals for a full B -physics program late in this decade.

8 References

- [1] BCD Collaboration, *Proposal for a B-Physics Experiment at TEV I: The μ BCD*, submitted to Fermilab (Oct. 8, 1990).
- [2] P. Lebrun, *A Bottom Collider Vertex Detector Design, Monte-Carlo Simulation and Analysis Package*, FNAL-TM-1682 (Oct. 1, 1990).

- [3] H. Mulderink, N. Michels, and H. Jöstlein, *Mechanical and Thermal behavior of a Prototype Support Structure for a Large Silicon Vertex Detector (BCD)*, Fermilab TM-1616 (August 23, 1989).
- [4] H. Jöstlein and J. Miller, *Heat Resistance and Air Pressure Drop in a Model of the BCD Silicon Vertex Detector*, BCD Internal Note RP-211 (Jan. 9, 1990).
- [5] H. Jöstlein and H. Mulderink, *Continued Studies of the Mechanical and Thermal behavior of a Prototype Support Structure for a Large Silicon Vertex Detector (BCD)*, Fermilab TM-1685 (Oct. 1990).
- [6] C. Lindenmeyer, *Proposed Method of Assembly for the BCD Silicon Strip Vertex Detector Modules*, Fermilab TM-1627 (Oct. 16, 1989).
- [7] R. Yarema, *BVX Workshop Summary*, BCD-RP-207 (Nov. 28, 1989).
- [8] H. Attias *et al.*, *Beam Tests of Silicon Microstrip Detectors with VLSI Readout*, to appear in the Proceedings of the IEEE Detector Conference (Crystal City, Oct. 1990).
- [9] P. Skubic *et al.*, *Vertex Detector Technology for the SSC*, to appear in the Proceedings of the SSC Detector Symposium (Ft. Worth, Oct. 1990).
- [10] J.D. Bjorken, *Estimates of Decay branching Ratios for Hadrons Containing Charm and Bottom Quarks*, (1986), unpublished.
- [11] BCD Collaboration, *Bottom Collider Detector Expression of Interest*, submitted to the SSC (May 25, 1990).
- [12] P. Krawczyk, D. London, R.D. Peccei, and H. Steger, *Predictions of the CKM Model for CP Asymmetries in B Decay*, Nucl. Phys. B307, 19 (1988).
- [13] A. Einstein, B. Podolsky, and N. Rosen, *Can Quantum-Mechanical Description of Physical Reality be Considered Complete?*, Phys. Rev. 47, 777 (1935).
- [14] A.B. Carter and A.I. Sanda, *CP Nonconservation in Cascade Decays of B Mesons*, Phys. Rev. Lett. 45, 952 (1980); *CP Violation in B-Meson Decays*, Phys. Rev. D 23, 1567 (1981). For algebraic details, see also I.I. Bigi and A.I. Sanda, *Notes on the Observability of CP Violations in B Decays*, Nucl. Phys. B193, 85 (1981).
- [15] See also J. Liu and L. Wolfenstein, *Superweak Contribution to B^0 - \bar{B}^0 Mixing*, Phys. Lett. 197B, 536 (1987).

